Inorg. Chem. **2006**, *45*, 2857–2865

Structures, Photoluminescence, Up-Conversion, and Magnetism of 2D and 3D Rare-Earth Coordination Polymers with Multicarboxylate Linkages

Jin Yang, Qi Yue, Guo-Dong Li, Jun-Jun Cao, Guang-Hua Li, and Jie-Sheng Chen*

State Key Laboratory of Inorganic Synthesis and Preparative Chemistry, College of Chemistry, Jilin University, Changchun 130012, People's Republic of China

Received September 12, 2005

Four new rare-earth compounds, $[Eu(NDC)_{1.5}(DMF)_2]$ (**1**), $[Nd_2(NDC)_3(DMF)_4]\cdot H_2O$ (**2**), $[La_2(NDC)_3(DMF)_4]\cdot 0.5H_2O$ (**3**), and $[Eu(BTC)(H_2O)]$ (**4**), where NDC = 1,4-naphthalenedicarboxylate, BTC = 1,3,5-benzenetricarboxylate, and DMF = *N*,*N*-dimethylformamide, have been synthesized through preheating and cooling-down crystallization. Compounds **1**–**3** possess similar 2D structures, in which the NDC ligands link M^{III} (M = La, Nd, and Eu) ions of two adjacent double chains constructed by NDC ligands and dinuclear M^{III} building units. In compound **4**, the Eu^{III} ion is seven-coordinated by O atoms from six BTC ligands and one terminal water molecule in a distorted pentagonal-bipyramidal coordination environment. If the BTC ligand and the Eu^{III} ion are regarded as six-connected nodes, respectively, the structure of compound **4** can be well described as a 3D six-connected net. Furthermore, compounds **1** and **4** exhibit strong red luminescence upon 355-nm excitation. Compound **2** displays interesting emissions in the near-IR region, and yellow (580 nm) pumping of this compound results in UV and intense blue emissions through an up-conversion process. The magnetic properties of compounds **1**, **2**, and **4** have been studied through measurement of their magnetic susceptibilities over the temperature range of 4–300 K.

Introduction

Recently, 4f and 5f metal coordination compounds have attracted increasing attention because of their interesting properties such as magnetism,[1] photoluminescence,[2] photovoltaic conversion,[3] and photocatalysis.[4] Lanthanide (4f) complexes usually exhibit intense luminescence and are potentially applicable for the manufacture of fluorescent probes and electroluminescent devices.[5] The optical properties of lanthanide ions are different from those of other metal ions and molecular species because they absorb and emit light over narrow wavelength ranges with high quantum yields.[6] Among the lanthanide ions, Eu^{III} and Nd^{III} are two of the most important luminescent centers. Eu^{III} complexes have been regarded as attractive for use as visible luminescent materials because of their strong red emissions (615 nm), while Nd^{III} complexes emitting in the near-IR region (800−1700 nm) are the most popular near-IR luminescent compounds for application in laser systems.[7] Another interesting feature of Nd^{III} compounds is their frequency up-conversion of IR radiation into the visible region, and thus Nd^{III}-containing complexes may also find application in two-

* To whom correspondence should be addressed. E-mail: chemcj@mail.jlu.edu.cn. Tel.: +86-431-5168662. Fax: +86-431-5168624.

(1) (a) Yue, Q.; Yang, J.; Li, G. H.; Li, G. D.; Xu, W.; Chen, J. S.; Wang, S. N. *Inorg. Chem.* **2005**, *44*, 5241. (b) Zheng, X. J.; Jin, L. P.; Gao, S. *Inorg. Chem.* **2004**, *43*, 1600. (c) Kido, T.; Ikuta, Y.; Sunatsuki, Y.; Ogawa, Y.; Matsumoto, N.; Re, N. *Inorg. Chem.* **2003**, *42*, 398. (d) Ma, B. Q.; Zhang, D. S.; Gao, S.; Jin, T. Z.; Yan, C. H.; Xu, G. X. *Angew. Chem., Int. Ed.* **2000**, *39*, 3644.

(2) (a) Yu, Z. T.; Li, G. H.; Jiang, Y. S.; Xu, J. J.; Chen, J. S. *J. Chem Soc., Dalton Trans.* **2003**, *22*, 4219. (b) Bassett, A. P.; Magennis, S. W.; Glover, P. B.; Lewis, D. J.; Spencer, N.; Parsons, S.; Williams, R. M.; Cola, L. D.; Pikramenou, Z. *J. Am. Chem. Soc.* **2004**, *126*, 9413. (c) Reineke, T. M.; Eddaoudi, M.; Fehr, M.; Kelley, D.; Yaghi, O. M. *J. Am. Chem. Soc.* **1999**, *121*, 1651. (d) Serre, C.; Stock, N.; Bein, T.; Férey, G. *Inorg. Chem.* **2004**, *43*, 3159. (e) Vicentini, G.; Zinner, L. B.; Zukerman-Schpector, J.; Zinner, K. *Coord. Chem. Rev.* **2000**, *196*, 353.

(3) Chen, W.; Yuan, H. M.; Wang, J. Y.; Liu, Z. Y.; Yang, M. Y.; Chen, J. S. *J. Am. Chem. Soc.* **2003**, *125*, 9266.

(4) (a) Yu, Z. T.; Liao, Z. L.; Jiang, Y. S.; Li, G. H.; Chen, J. S. *Chem.—Eur. J.* **2005**, *11*, 2642. (b) Yu, Z. T.; Liao, Z. L.; Jiang, Y. S.; Li, G. H.; Li, G. D.; Chen, J. S. *Chem Commun.* **2004**, 1814.

(5) (a) Buünzli, G. J. C.; Piguet, C. *Chem. Rev.* **2002**, *102*, 1897. (b) Tsukube, H.; Shinoda, S. *Chem. Rev.* **2002**, *102*, 2389. (c) Capecchi, S.; Renault, O.; Moon, D. G.; Halim, M.; Etchells, M.; Dobson, P. J.; Salata, O. V.; Christou, V. *Adv. Mater.* **2000**, *12*, 1591. (d) Kido, J.; Okamoto, Y. *Chem. Rev.* **2002**, *102*, 2357.

(6) Sabbatini, N.; Guardigli, M.; Lehn, J. M. *Coord. Chem. Rev.* **1993**, *123*, 201.

10.1021/ic051557o CCC: $33.50
Published on Web 03/01/2006

photon fluorescence imaging.[8] Nevertheless, the photophysical properties of lanthanide complexes markedly depend on their structures, and therefore it is of great significance to obtain new structures of rare-earth compounds and to reveal the relationship between the structures and photophysical properties for these compounds.[9] In all types of rare-earth compounds, carboxylate anions with aromatic rings are widely used in the construction of high-dimensional lanthanide coordination polymers because these anions are able to act as bridging ligands in various ligating modes.[10]

Conventionally, the syntheses of rare-earth carboxylate compounds are carried out in aqueous media, where water molecules easily coordinate to the rare-earth centers and usually quench the luminescence intensity.[11] Moreover, aromatic carboxylic acids show low solubility in aqueous solution even under hydrothermal conditions because of the presence of conjugated aromatic rings, leading to difficulty in obtaining single crystals of rare-earth carboxylate materials. To obtain single crystals of lanthanide aromatic carboxylate complexes, we tried an unconventional synthetic approach in which *N*,*N*-dimethylformamide (DMF) was used as the solvent and the crystallization was realized through a preheating and cooling-down route. We chose 1,4-naphthalenedicarboxylate (NDC) and 1,3,5-benzenetricarboxylate (BTC) as linkers and chelating ligands to coordinate to the rare-earth metals. Both the rodlike NDC and the starlike BTC molecules possess interesting features that are conducive to the formation of versatile coordination structures.[10a] First, the multicarboxylate groups on the molecules may be completely or partially deprotonated and, second, the carboxylate groups may not lie in the phenyl ring plane upon coordination to metal ions owing to space hindrance, and as a result, the molecules may connect metal ions in different directions. In this paper, we describe the successful synthesis of four new lanthanide compounds with extended structures, $[Eu(NDC)_{1.5}(DMF)_2]$ (**1**), $[Nd_2(NDC)_3(DMF)_4]\cdot H_2O$ (**2**), $[La_2(NDC)_3(DMF)_4]\cdot 0.5H_2O$ (**3**), and $[Eu(BTC)(H_2O)]$ (**4**) in the presence of DMF as the solvent, through the preheating and cooling-down crystallization approach. The photoluminescence, up-conversion property, and temperature-dependent magnetic behaviors of these compounds have also been investigated.

Experimental Section

Materials. $EuCl_3\cdot 6H_2O$, $NdCl_3\cdot 6H_2O$, and $LaCl_3\cdot 6H_2O$ were prepared by dissolving Eu_2O_3, Nd_2O_3, and La_2O_3, respectively, in hydrochloric acid followed by drying and crystallization. The H_2-NDC, H_3BTC, and other reagents of analytical grade were purchased commercially and used without further purification.

Synthesis of $[Eu(NDC)_{1.5}(DMF)_2]$ (1). $EuCl_3\cdot 6H_2O$ (0.122 g, 0.33 mmol) and H_2NDC (0.108 g, 0.5 mmol) were dissolved in DMF (10 mL). The resulting mixture was stirred for about 1 h at room temperature, sealed in a 23-mL Teflon-lined stainless steel autoclave, and heated at 80 °C for 3 days under autogenous pressure. Afterward, the reaction system was gradually cooled to room temperature at a rate of 15 °C h^{-1}. Colorless crystals of **1** suitable for single-crystal X-ray diffraction (XRD) analysis were collected from the final reaction system by filtration, washed several times with DMF, and dried in air at ambient temperature. Yield: 45% based on Eu^{III}. Elem and ICP anal. Calcd for $C_{24}H_{22}EuN_2O_8$: C, 46.61; H, 3.59; N, 4.53; Eu, 24.57. Found: C, 46.33; H, 3.83; N, 4.91; Eu, 24.81. IR (cm^{-1}): 2944 (w), 1656 (s), 1597 (m), 1474 (m), 1422 (s), 1364 (s), 1267 (w), 1106 (w), 846 (s), 794 (m), 678 (w), 568 (w), 438 (m).

Synthesis of $[Nd_2(NDC)_3(DMF)_4]\cdot H_2O$ (2). Compound **2** was prepared in the same way as that for **1** but using $NdCl_3\cdot 6H_2O$ (0.120 g, 0.33 mmol) and H_2NDC (0.108 g, 0.5 mmol) as the reactants. Rose-colored crystals were obtained in a 43% yield based on Nd^{III}. Elem and ICP anal. Calcd for $C_{48}H_{48}N_4Nd_2O_{17}$: C, 46.44; H, 3.90; N, 4.51; Nd, 23.24. Found: C, 46.17; H, 3.66; N, 4.72; Nd, 23.43. IR (cm^{-1}): 3423 (w), 2931 (w), 1653 (s), 1594 (m), 1476 (m), 1423 (s), 1364 (s), 1266 (w), 1104 (w), 846 (s), 792 (m), 681 (w), 566 (w), 435 (m).

Synthesis of $[La_2(NDC)_3(DMF)_4]\cdot 0.5H_2O$ (3). Compound **3** was prepared similarly, using $LaCl_3\cdot 6H_2O$ (0.118 g, 0.33 mmol) and H_2NDC (0.108 g, 0.5 mmol) as the reactants. Colorless crystals were obtained in a 56% yield based on La^{III}. Elem and ICP anal. Calcd for $C_{48}H_{47}La_2N_4O_{16.5}$: C, 47.19; H, 3.88; N, 4.59; La, 22.74. Found: C, 46.89; H, 3.56; N, 4.23; La, 22.96. IR (cm^{-1}): 3427 (w), 2933 (w), 1657 (s), 1593 (m), 1474 (m), 1421 (s), 1365 (s), 1266 (w), 1106 (w), 845 (s), 792 (m), 680 (w), 569 (w), 439 (m).

Synthesis of $[Eu(BTC)(H_2O)]$ (4). $EuCl_3\cdot 6H_2O$ (0.122 g, 0.33 mmol) and H_3BTC (0.070 g, 0.33 mmol) were dissolved in DMF (10 mL). The resulting solution was stirred for about 1 h at room temperature, sealed in a 23-mL Teflon-lined stainless steel autoclave, and heated at 85 °C for 5 days under autogenous pressure. Afterward, the reaction system was gradually cooled to room temperature at a rate of 15 °C h^{-1}. Colorless crystals of **4** suitable for single-crystal XRD analysis were collected from the final reaction system by filtration and dried in air at ambient temperature. Yield: 39% based on Eu^{III}. Elem and ICP anal. Calcd for $C_{4.5}H_{2.5}Eu_{0.5}O_{3.5}$: C, 28.67; H, 1.34; Eu, 40.30. Found: C, 28.92; H, 1.19; Eu, 40.91. IR (cm^{-1}): 3397 (m), 2769 (w), 1616 (s), 1559 (s), 1442 (m), 1369 (s), 1111 (w), 769 (m), 704 (w), 529 (w).

General Characterization and Physical Measurements. The IR spectra were recorded within the 400−4000-cm^{-1} region on a Bruker IFS 66V/S Fourier transform IR (FTIR) spectrometer using KBr pellets. The C, H, and N elemental analysis was conducted on a Perkin-Elmer 240C element analyzer, whereas the inductively coupled plasma (ICP) analysis was performed on a Perkin-Elmer Optima 3300DV ICP spectrometer. The powder XRD data were collected on a Siemens D5005 diffractometer with Cu Kα radiation

(7) (a) Beeby, A.; Faulkner, S. *Chem. Phys. Lett.* **1997**, *266*, 116. (b) Imbert, D.; Cantuel, M.; Bünzli, J. C. G.; Bernardinelli, G.; Piguet, C. *J. Am. Chem. Soc.* **2003**, *125*, 15698. (c) Weber, M. J. In *Lanthanide and Actinide Chemistry and Spectroscopy*; Edelstein, N. M., Ed.; ACS Symposium Series 131; American Chemical Society: Washington, DC, 1980; p 275. (d) Ryo, M.; Wada, Y.; Okubo, T.; Hasegawa, Y.; Yanagida, S. *J. Phys. Chem. B* **2003**, *107*, 11302.

(8) (a) Patra, A.; Friend, C. S.; Kapoor, R.; Prasad, P. N. *Chem. Mater.* **2003**, *15*, 3650. (b) Wang, X.; Kong, X.; Shan, G.; Yu, Y.; Sun, Y.; Feng, L.; Chao, K.; Lu, S.; Li, Y. *J. Phys. Chem. B* **2004**, *108*, 18408.

(9) Deun, R. V.; Fias, P.; Nockemann, P.; Schepers, A.; Parac-Vogt, T. N.; Hecke, K. V.; Meervelt, L. V.; Binnemans, K. *Inorg. Chem.* **2004**, *43*, 8461.

(10) (a) Wang, Z.; Kravtsov, V. C.; Zaworotko, M. J. *Angew. Chem., Int. Ed.* **2005**, *44*, 2. (b) Lin, Z.; Jiang, F.; Chen, L.; Yuan, D.; Hong, M. *Inorg. Chem.* **2005**, *44*, 73. (c) Zheng, X.-J.; Jin, L. P.; Gao, S.; Lu, S. Z. *New J. Chem.* **2005**, *6*, 798. (d) Rosi, N. L.; Kim, J.; Eddaoudi, M.; Chen, B.; O'Keeffe, M.; Yaghi, O. M. *J. Am. Chem. Soc.* **2005**, *127*, 1504. (e) Kim, Y. J.; Jung, D. Y. *Chem. Commun.* **2002**, 908. (f) Ghosh, S. K.; Bharadwaj, P. K. *Inorg. Chem.* **2004**, *43*, 2293. (g) Ghosh, S. K.; Bharadwaj, P. K. *Inorg. Chem.* **2003**, *42*, 8250.

(11) Bellusci, A.; Barberio, G.; Crispini, A.; Ghedini, M.; Deda, M. L.; Pucci, D. *Inorg. Chem.* **2005**, *44*, 1818.

Table 1. Crystallographic Data for Complexes **1**−**4**

	1	**2**	**3**	**4**
empirical formula	$C_{24}H_{22}EuN_2O_8$	$C_{48}H_{48}N_4Nd_2O_{17}$	$C_{48}H_{47}La_2N_4O_{16.5}$	$C_{4.5}H_{2.5}Eu_{0.5}O_{3.5}$
fw	618.40	1241.38	1221.72	188.55
space group	$P\bar{1}$	$P\bar{1}$	$P\bar{1}$	$P4_322$
a [Å]	11.3894(13)	11.465(2)	11.5541(9)	10.3627(15)
b [Å]	11.5985(18)	11.704(2)	11.7802(10)	10.3627(15)
c [Å]	11.7351(17)	23.342(5)	23.5745(15)	14.332(3)
α [deg]	77.968(10)	79.08(3)	79.366(5)	90
β [deg]	61.694(8)	87.29(3)	87.169(5)	90
γ [deg]	86.258(9)	62.07(3)	62.000(5)	90
V [Å^3]	1333.8(3)	2714.2(9)	2781.9(4)	1539.1(4)
Z	2	2	2	8
ρ [g cm^{-3}]	1.540	1.519	1.459	1.627
μ [mm^{-1}]	2.397	1.961	1.581	4.089
GOF on F^2	0.906	1.078	0.915	0.953
R [$I > 2\sigma(I)$][a]	R1 = 0.0601	R1 = 0.0512	R1 = 0.0518	R1 = 0.0404
	wR2 = 0.1117	wR2 = 0.1536	wR2 = 0.1019	wR2 = 0.0904

[a] $R1 = \sum||F_o| - |F_c||/\sum |F_o|$; $wR2 = \{\sum[w(F_o^2 - F_c^2)^2]/\sum[w(F_o^2)]^2\}^{1/2}$.

(λ = 1.5418 Å), and the recording speed was 0.3° min^{-1} over the 2θ range of 4−40° at room temperature. The simulated and experimental powder XRD patterns of compounds **1**−**4** are shown in the Supporting Information (Figures S5−S8). Temperature-dependent magnetic susceptibility data for polycrystalline compounds **1**, **2**, and **4** were obtained on a Quantum Design MPMS-XL SQUID magnetometer under an applied field of 1000 Oe over the temperature range of 4−300 K. The visible luminescent properties of compounds **1** and **4** were measured on a Perkin-Elmer LS55 spectrometer. The near-IR emission spectrum of compound **2** was recorded on an Edinburgh Analytical Instruments FLS920 equipped with a laser diode from the PicoQuant Company as the light source, whereas the up-conversion spectrum of this compound was obtained using a tunable pulsed laser (Continuum Sunlite OPO). The luminescent lifetime was measured with a TR550 (J-Y Company) upon excitation with a Nd:YAG laser.

X-ray Crystallography. Crystallographic data of compounds **2** and **4** were collected on a Rigaku RAXIS−RAPID single-crystal diffractometer equipped with a narrow-focus, 5.4-kW sealed-tube X-ray source (graphite-monochromated Mo Kα radiation with λ = 0.710 73 Å) at a temperature of 20 ± 2 °C. The data processing was accomplished with the PROCESS-AUTO processing program. Crystallographic data for **1** and **3** were recorded at room temperature on a Bruker-AXS Smart CCD diffractometer equipped with a normal-focus, 2.4-kW X-ray source (graphite-monochromated Mo Kα radiation with λ = 0.710 73 Å) operating at 50 kV and 40 mA with increasing ω (width of 0.3° and exposure time of 30 s frame^{-1}). All of the structures were solved by direct methods using the program *SHELXS-97*[12] and refined by full-matrix least-squares techniques against F^2 using the *SHELXTL-97*[13] crystallographic software package. All non-H atoms were easily found from the difference Fourier map and refined anisotropically, whereas the H atoms of the organic molecules were placed by geometrical considerations and were added to the structure factor calculation. The detailed crystallographic data and structure refinement parameters for **1**−**4** are summarized in Table 1.

Results and Discussion

Selected bond distances and angles for compounds **1**−**4** are listed in Tables S1−S4 (see the Supporting Information). The structures of compounds **2** and **3** are similar to that of compound **1**, and therefore only the structures of **1** and **4** will be described in detail. The experimental powder XRD and elemental and ICP analyses of compounds **1**−**4** were performed before their properties were measured. The elemental and ICP analysis results for all of the compounds well correspond to the data calculated from the single-crystal structure formulas (see the Experimental Section). The experimental powder XRD patterns are also in good agreement with the corresponding simulated ones (Figures S5−S8 in the Supporting Information) except for the relative intensity variation because of preferred orientations of the crystals. Therefore, the phase purity of the as-synthesized products is substantiated.

Structural Description of 1. The asymmetric unit for compound **1** is shown in Figure 1a. It is seen that each Eu^{III} center is coordinated by nine O atoms from six NDC anions (O1, O2, O5, O4A, O3A, O3B, and O6A) and two DMF molecules (O7 and O8). The Eu−O(carboxylate) bond distances ranging from 2.371 to 2.654 Å and the Eu−O(DMF) bond distances from 2.447 to 2.460 Å are similar to previously reported Eu−O lengths.[14] It is well-known that the two possible ground-state geometries for a nine-coordination polyhedron are the symmetrical tricapped trigonal prism with D_{3h} symmetry and the monocapped square antiprism with C_{4v} symmetry.[15] The polyhedron of the Eu^{III} coordination sphere for compound **1** is best described as a distorted tricapped trigonal prism (Figure 1b).

In compound **1**, the NDC anions display two orientations, and the dihedral angle between the naphthalene rings of the two oriented NDC molecules is 159.5°. For convenience, the NDC anions containing the O atoms labeled O1 and O5 (Figure 1a) are designated as NDC1 and NDC2, respectively. In coordination mode 1 (for NDC1), one carboxylate moiety chelates one Eu^{III} ion, while the other carboxylate group links

(12) Sheldrick, G. M. *SHELXS-97, Programs for X-ray Crystal Structure Solution*; University of Göttingen: Göttingen, Germany, 1997.
(13) Sheldrick, G. M. *SHELXL-97, Programs for X-ray Crystal Structure Refinement*; University of Göttingen: Göttingen, Germany, 1997.
(14) (a) Li, J. R.; Bu, X. H.; Zhang, R. H.; Duan, C. Y.; Wong, K. M. C.; Yam, V. W. W. *New J. Chem.* **2004**, *28*, 261. (b) Bu, X.-H.; Weng, W.; Du, M.; Chen, W.; Li, J.-R.; Zhang, R.-H.; Zhao, L.-J. *Inorg. Chem.* **2002**, *41*, 1007.
(15) Hou, H.; Wei, Y.; Song, Y.; Fan, Y.; Zhu, Y. *Inorg. Chem.* **2004**, *43*, 1323.

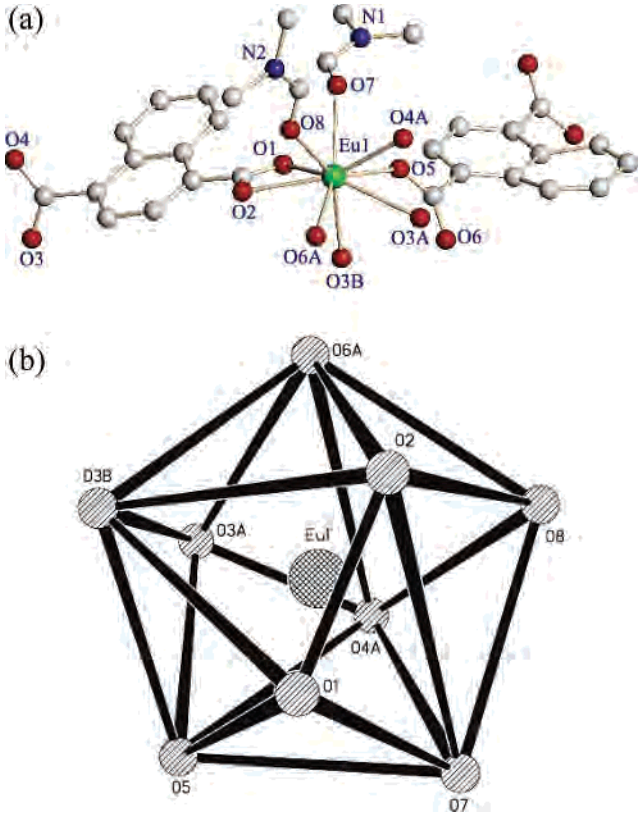

Figure 1. View of the asymmetric unit of compound **1** (all H atoms are omitted for clarity) (a) and the distorted tricapped trigonal-prismatic coordination polyhedron of the Eu^{III} ion (b).

Chart 1. Coordination Modes of the NDC and BTC Molecules in Compounds **1**−**4**

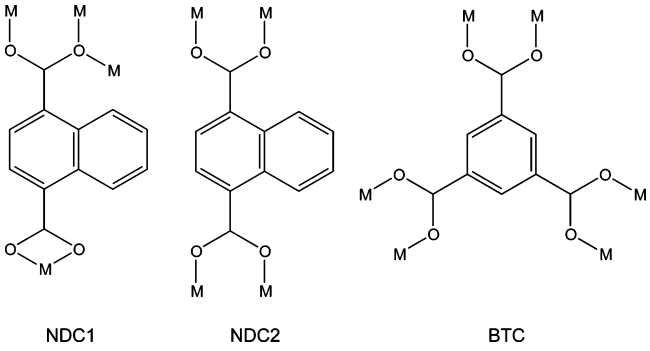

three Eu^{III} ions. In mode 2 (for NDC2), each carboxylate moiety bridges two adjacent Eu^{III} ions (Chart 1).

The dinuclear Eu^{III} units in compound **1** are further connected through NDC ligands, resulting in a unique 2D layer network. First, the NDC1 ligands link the dimer units to form 1D double-chain structures (Figure 2), and the distance between adjacent dimer units in the chain is 12.25 Å. Second, the NDC2 ligands link the Eu^{III} units of two adjacent chains to form the 2D layers (Figure 2). Moreover, the layers are packed in a parallel fashion to form a 3D supramolecular structure through $\pi-\pi$ interactions of adjacent naphthalene rings.

The structures of compounds **2** and **3** are similar to that of compound **1**. Nevertheless, a small difference exists for these three compounds. As shown in Tables S1−S4 (see the Supporting Information), the metal−O bond distances and

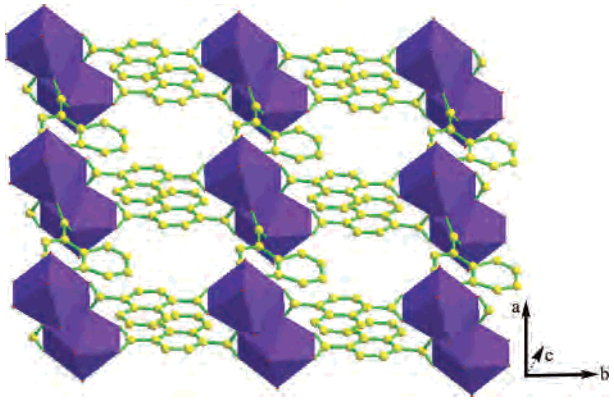

Figure 2. 2D network structure of **1** viewed along the *c* axis.

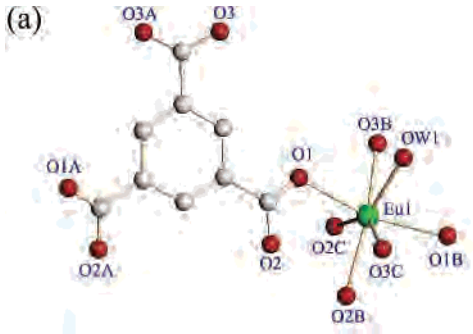

Figure 3. View of the asymmetric unit of compound **4** (all H atoms are omitted for clarity) (a) and the distorted pentagonal-bipyramidal coordination sphere of the Eu^{III} ion (b).

angles for compounds **1**−**3** are observed to vary from compound to compound because the radii of M^{III} (M = La, Nd, and Eu) are in the order **1** < **2** < **3**. In addition, whereas compound **1** is completely water-free, compounds **2** and **3** contain water molecules occluded in the voids of the structural networks. It is believed that these water molecules originate from the starting reactants $NdCl_3 \cdot 6H_2O$ and $LaCl_3 \cdot 6H_2O$. Nevertheless, they are not coordinated to the metal ions of the final products in the presence of DMF as the predominant solvent in the reaction system.

Structural Description of 4. The asymmetric unit for compound **4** is shown in Figure 3a. Each Eu^{III} ion in **4** is seven-coordinated by O atoms from six BTC ligands (O1, O1B, O2B, O2C, O3B, and O3C) and one terminal water

molecule (Ow1) in a distorted pentagonal-bipyramidal coordination sphere, in which the four O atoms from four BTC anions (O2B, O2C, O3B, and O3C) and one O atom from the water molecule (Ow1) make up the basal plane, while the axial positions are occupied by two O atoms (O1 and O1B) from another two BTC molecules (Figure 3b). The Eu−O(carboxylate) bond lengths vary from 2.321 to 2.369 Å, and the Eu−Ow1 distance is 2.469 Å. The O−Eu^{III}−O bond angles range from 69 to 161.3°.

The interesting feature of compound **4** is the presence of helical strands in the structure. As depicted in Figure 4, the BTC ligands bridge adjacent Eu^{III} ions to form three-stranded helical chains running along the crystallographic 4_3 axis. The occurrence of helical strands in compound **4** is attributable to the steric orientation of the carboxylate groups of BTC. The helical chains are further linked with each other through the BTC ligands to form a 3D framework. In addition, unlike the previously reported 3D $Eu_3(H_2O)(OH)_6(BTC)_3 \cdot 3H_2O$ compound whose structure consists of $[Eu_3(OH)_6]_n$ sheets linked together by BTC ligands,[16] compound **4** is composed of mononuclear Eu^{III} cations bridged by BTC ligands in all three directions. Each carboxylate group in **4** connects two Eu^{III} ions in a bidentate manner, and each ligand bridges six adjacent Eu^{III} ions through their carboxylate O atoms. Thus, if the BTC ligand and the seven-coordinated Eu^{III} ion are regarded as the six-connected nodes, the framework topology of compound **4** can be regarded as of the 3D six-connected net.[17] This observation suggests that the flexible coordination mode of the BTC ligand in combination with the high coordination number of Eu^{III} favors the formation of a highly connected net.

It is worthwhile to note that, although the DMF molecules do not coordinate to the Eu^{III} ions in compound **4**, they play an important role in the crystallization process of the compound. In the absence of DMF, no crystals of compound **4** were obtained under similar synthetic conditions. The presence of DMF improves the solubility of the ligands and makes the crystal growth more homogeneous.

Photoluminescence. The solid-state photoluminescent spectra of compounds **1**, **2**, and **4** were recorded at room temperature. As shown in Figure 5a, the NDC ligand exhibits a fluorescent emission band at 472 nm (λ_{ex} = 392 nm), while the free BTC ligand shows an emission band at 380 nm (λ_{ex} = 334 nm). The emission bands for these two free ligands are attributable to the $\pi^* \rightarrow$ n transitions.[18] Compound **3** contains a nonemissive La^{III} ion, and this material shows a very weak emission band at 533 nm (λ_{ex} = 392 nm), which is believed to arise from charge-transfer transition between the NDC ligand and the central La^{III} ion.[18] The photoluminescent spectra of compounds **1**, **2**, and **4** exhibit emission bands characteristic of the corresponding luminescent lanthanide ions, whereas the emissions arising from the free ligands are not observable for these three compounds. The absence of ligand-based emission suggests energy transfer from the ligands to the lanthanide center during photoluminescence.[18c] Compounds **1** and **4** (both contain Eu^{III} ions)

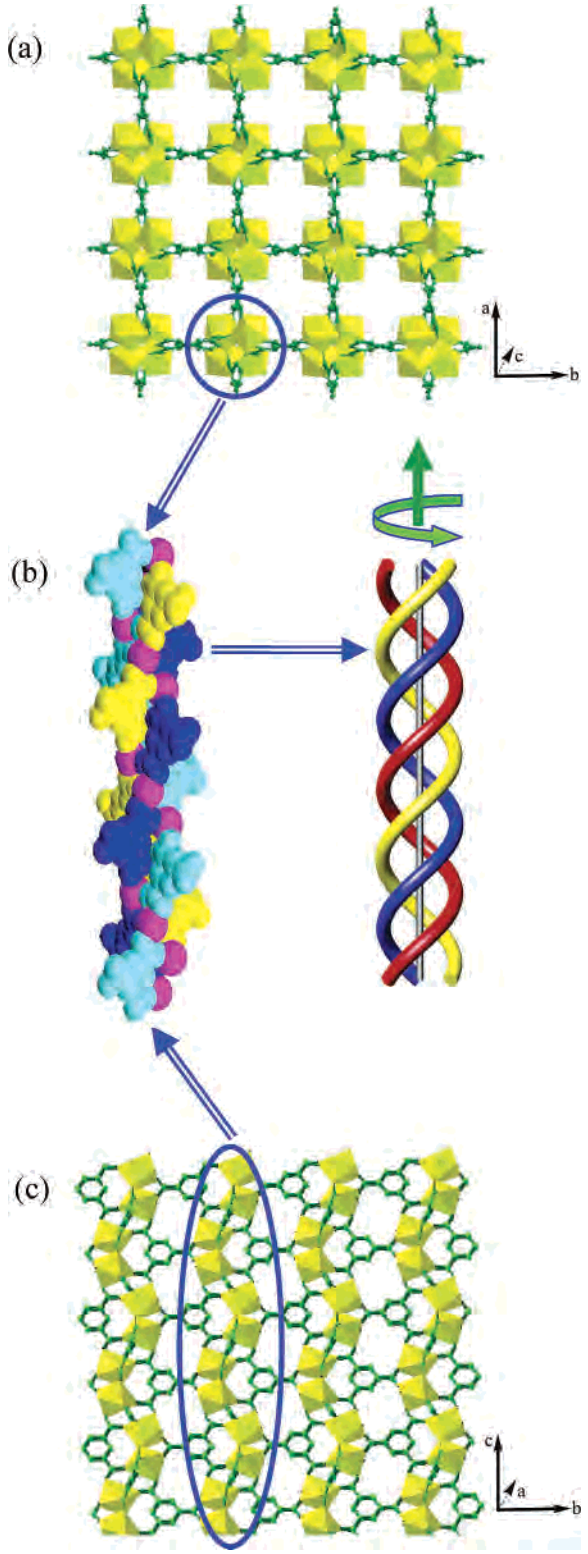

Figure 4. 3D framework structure of **4** viewed along the *c* axis (a), the three-stranded helical structure running along the crystallographic 4_3 axis (b), and the 3D structure of **4** viewed along the *a* axis (c).

(16) Serre, C.; Férey, G. *J. Mater. Chem.* **2002**, *12*, 3053.
(17) (a) Batten, S. R.; Robson, R. *Angew. Chem., Int. Ed.* **1998**, *37*, 1460. (b) Chen, X. Y.; Zhao, B.; Shi, W.; Xia, J.; Cheng, P.; Liao, D. Z.; Yan, S. P.; Jiang, Z. H. *Chem. Mater.* **2005**, *17*, 2866. (c) Ma, J. F.; Yang, J.; Zheng, G. L.; Li, L.; Liu, J. F. *Inorg. Chem.* **2003**, *42*, 7531.
(18) (a) Chen, W.; Wang, J. Y.; Chen, C.; Yue, Q.; Yuan, H. M.; Chen, J. S.; Wang, S. N. *Inorg. Chem.* **2003**, *42*, 944. (b) Wang, X.; Qin, C.; Wang, E.; Li, Y.; Hao, N.; Hu, C.; Xu, L. *Inorg. Chem.* **2004**, *43*, 1850. (c) Sun, Y.-Q.; Zhang, J.; Chen, Y.-M.; Yang, G.-Y. *Angew. Chem., Int. Ed.* **2005**, *44*, 5814.

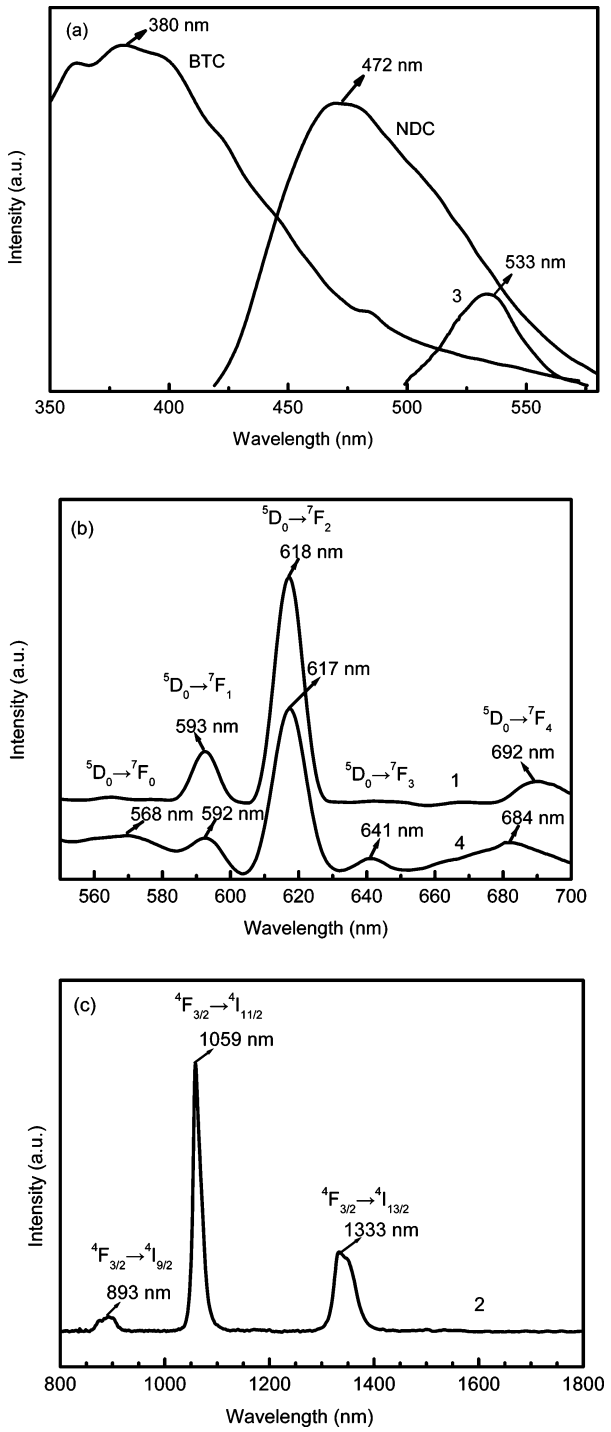

Figure 5. Solid-state emission spectra for a free NDC ligand excited at 392 nm, the BTC ligand excited at 334 nm, and compound **3** excited at 392 nm (a), for **1** excited at 355 nm, for **4** excited at 355 nm (b), and for **2** excited at 488 nm (c). All of the spectra were recorded at room temperature.

emit red light upon excitation at 355 nm, and their luminescence spectra are depicted in Figure 5b. These emission bands arise from $^5D_0 \rightarrow {}^7F_J$ ($J = 0-4$) transitions, typical of Eu^{III} ions.[19] For **1**, the $^5D_0 \rightarrow {}^7F_0$ and $^5D_0 \rightarrow {}^7F_3$ transitions are too weak to be observed, but the symmetry-forbidden emission $^5D_0 \rightarrow {}^7F_0$ at 568 nm can be found for solid **4**. It is well-known that the transition $^5D_0 \rightarrow {}^7F_0$ is strictly forbidden in a field of high symmetry and, therefore, the Eu^{III} ion in **4** should occupy sites with a low symmetry and no inversion center should be present for these sites, in agreement with the crystal structural analysis.[2e,20] The $^5D_0 \rightarrow {}^7F_1$ transition (593 nm for **1** and 592 nm for **4**) corresponds to a magnetic dipole transition, and the intensities of this emission for both **1** and **4** are medium-strong. The most intense emissions in the luminescent spectra are the $^5D_0 \rightarrow {}^7F_2$ transitions at 618 and 617 nm for **1** and **4**, respectively, which are the so-called hypersensitive transitions and are responsible for the brilliant-red emission of these complexes.[21] The $^5D_0 \rightarrow {}^7F_3$ transition at 641 nm is observed for **4**, whereas it is nearly invisible for compound **1**. Compound **2** has no emission in the visible region. However, this material shows distinct emissions in the near-IR region (Figure 5c). Near-IR-emitting materials based on rare-earth compounds have attracted considerable attention recently because they are promising candidates for active components in near-IR-luminescent optical devices.[22] The profiles of the emission bands for **2** are in agreement with previously reported spectra of Nd^{III} complexes.[23] Under an excitation of 488 nm, compound **2** displays a strong emission band at 1059 nm ($^4F_{3/2} \rightarrow {}^4I_{11/2}$), an emission band at 893 nm ($^4F_{3/2} \rightarrow {}^4I_{9/2}$) with a much lower intensity, and a very weak band at 1333 nm ($^4F_{3/2} \rightarrow {}^4I_{13/2}$).[23]

The luminescence decay curves of complexes **1** and **4** were obtained at room temperature. The decay curves are well fitted into a single-exponential function as $I = I_0 \exp(-t/\tau)$, where I and I_0 are the luminescent intensities at times t and 0 and τ is defined as the luminescent lifetime, indicating that all of the Eu^{III} ions occupy the same average local environment.[24] As shown in Figure 6, the luminescence lifetimes of compounds **1** and **4** are slightly different. The one for **1** is about 1.0 ms (Figure 6a), whereas that for **2** is about 0.84 ms (Figure 6b). This difference in lifetimes for the two compounds may result from the presence of

(19) (a) Lenaerts, P.; Driesen, K.; Deun, R. V.; Binnemans, K. *Chem. Mater*. **2005**, *17*, 2148. (b) He, Z.; Gao, E. Q.; Wang, Z. M.; Yan, C. H.; Kurmoo, M. *Inorg. Chem*. **2005**, *44*, 862. (c) Wang, Y.; Zheng, X.; Zhuang, W.; Jin, L. *Eur. J. Inorg. Chem.* **2003**, 3572.

(20) (a) Kim, Y. J.; Suh, M.; Jung, D. Y. *Inorg. Chem.* **2004**, *43*, 245. (b) Serre, C.; Pelle, F.; Gardant, N.; Férey, G. *Chem. Mater*. **2004**, *16*, 1177.

(21) (a) de Bettencourt-Dias, A. *Inorg. Chem*. **2005**, *44*, 2737. (b) Law, G. L.; Wong, K. L.; Zhou, X.; Wong, W. T.; Tanner, P. A. *Inorg. Chem*. **2005**, *44*, 4142.

(22) (a) Curry, R. J.; Gillin, W. P. *Appl. Phys. Lett.* **1999**, *75*, 1380. (b) Curry, R. J.; Gillin, W. P.; Knights, A. P.; Gwilliam, R. *Appl. Phys. Lett.* **2000**, *77*, 2271. (c) Khreis, O. M.; Curry, R. J.; Somerton, M.; Gillin, W. P. *J. Appl. Phys.* **2000**, *88*, 777. (d) Guo, X.; Zhu, G.; Fang, Q.; Xue, M.; Tian, G.; Sun, J.; Li, X.; Qiu, S. *Inorg. Chem*. **2005**, *44*, 3850.

(23) (a) Castro, A.; Enjalbert, R.; Lloyd, D.; Rasines, I.; Galy, J. *J. Solid State Chem.* **1990**, *85*, 100. (b) Tarasov, I. V.; Dolgikh, V. A.; Aksel'rud, L. G.; Berdonosov, P. S.; Ponovkin, B. A. *Zh. Neorg. Khim.* **1996**, *41*, 1243. (c) Nikiforov, G. B.; Kusainova, A. M.; Berdonosov, P. S.; Dolgikh, V. A.; Lightfoot, P. *J. Solid State Chem.* **1999**, *146*, 473. (d) Berdonosov, P. S.; Charkin, D. O.; Kusainova, A. M.; Hervoches, C. H.; Dolgikh, V. A.; Lightfoot, P. *Solid State Sci.* **2000**, *2*, 553. (e) Song, J. L.; Mao, J. G. *Chem.—Eur. J.* **2005**, *11*, 1417.

(24) (a) Ma, J.-F.; Yang, J.; Li, S.-L.; Song, S.-Y.; Zhang, H.-J.; Wang, H.-S.; Yang, K.-Y. *Cryst. Growth Des.* **2005**, *5*, 807. (b) Pang, X.; Sun, H.; Zhang, Y.; Shen, Q.; Zhang, H. *Eur. J. Inorg. Chem.* **2005**, 1487. (c) Choppin, G. R.; Peterman, D. R. *Coord. Chem. Rev*. **1998**, *174*, 283. (d) Bartelemy, P. P.; Choppin, G. R. *Inorg. Chem.* **1989**, *28*, 3354.

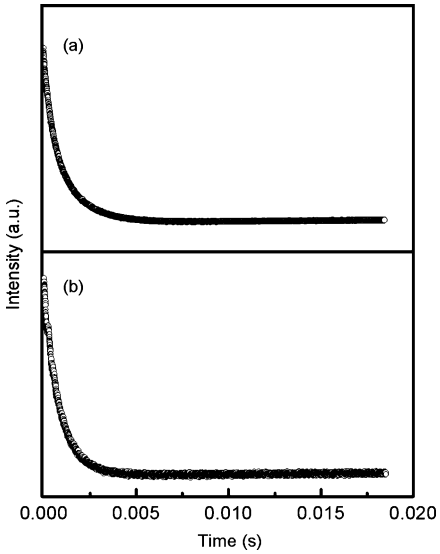

Figure 6. Luminescence decay curves for compound **1** ($\lambda_{ex} = 355$ nm; $\lambda_{em} = 618$ nm) (a) and for compound **4** ($\lambda_{ex} = 355$ nm; $\lambda_{em} = 617$ nm) (b).

coordinating water molecules in **4**, the vibration of which can effectively remove the electronic energy of excited Eu^{III} ions.[24]

Up-Conversion Property. Since the early reviews by Auzel and Wright about up-conversion processes, there has been extensive interest in up-conversion processes, up-conversion materials, and up-conversion applications,[25] and the search for new up-conversion compounds is one of the fundamental studies. Rare-earth-containing compounds have been found to be promising materials for up-conversion applications. However, most of the up-conversion rare-earth materials reported so far involve no organic ligands, and the use of Ln^{III} coordination polymers as up-conversion compounds has rarely appeared in the literature.[26] Therefore, it is highly desirable to explore the up-conversion properties of the rare-earth compounds we synthesized. Among compounds **1**−**4**, **2** contains Nd^{III} species, and this material exhibits interesting up-conversion emissions (Figure 7). A weak UV up-conversion emission at about 391.6 nm and a much stronger blue emission at about 449.5 nm show up for **2** upon pulse laser excitation at 580 nm. The reason behind the selection of the 580-nm excitation wavelength is that Nd^{III} compounds have intense absorption at 580 nm corresponding to transition $^4I_{9/2} \rightarrow {}^4G_{5/2}$, which is a hypersensitive band and satisfies the selection rules of $\Delta J = \pm 2$, $\Delta L = \pm 2$, and $\Delta S = 0$. Up-conversion emission peaks at these two wavelengths have also been observed for the Nd^{III}-doped $Bi_4Ge_3O_{12}$ and $Pb_5Al_3F_{19}$ crystals, respectively.[27]

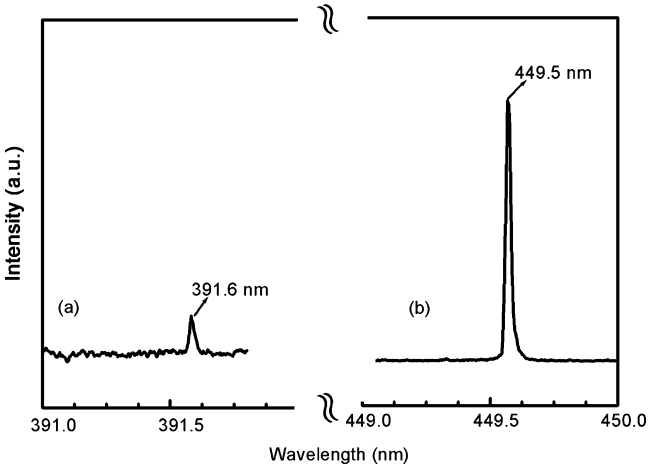

Figure 7. Up-conversion fluorescence spectrum of compound **2** recorded at room temperature (580-nm excitation).

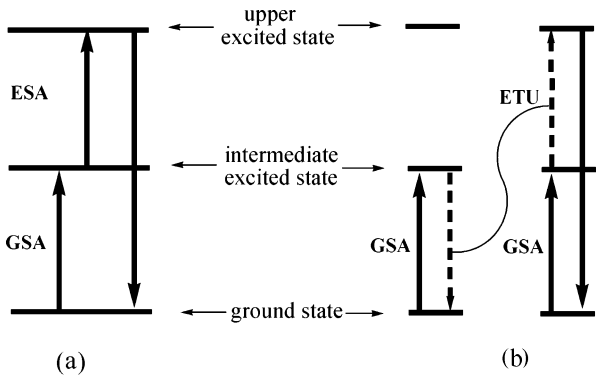

Figure 8. Schematic representation of two fundamental up-conversion mechanisms.

Figure 8 schematically shows the two most important up-conversion mechanisms in a simple three-level picture.[28] In Figure 8a, the emitting state is reached by a sequence of ground-state absorption (GSA) and excited-state absorption (ESA) steps. In this process (GSA/ESA), two photons are successively absorbed by one metal ion, and this mechanism is well documented for Ln^{III}-doped crystals and glasses.[29] Energy-transfer up-conversion (ETU) or GSA/ETU involves two ions in close proximity, and two metal ions are excited by GSA to their respective metastable intermediate states (Figure 8b).[30] This is followed by a nonradiative energy-transfer process resulting in one ion in the final excited state and the second one in the ground state. This mechanism is also well established in Ln^{III} systems.[31]

In the crystal structure of compound **2**, the distance between the dinuclear Nd^{III} ions bridged by the carboxylate O atom is 4.101 Å, which enables facile energy transfer between two optically active Nd^{III} ions, resulting in efficient

(25) (a) Auzel, F. *Acad. Sci. Paris* **1966**, 1016. (b) Wright, J. C. *Topics in Applied Physics: Radiationless Processes in Molecules and Condensed Phases*; Fong, F. K., Ed.; Springer: Berlin, 1976; pp 239−295. (c) Layne, B.; Lowdermilk, W. H.; Weber, M. J. *Phys. Rev. B* **1977**, *16*, 10.

(26) (a) Auzel, F. *Chem. Rev*. **2004**, *104*, 139. (b) Gamelin, D. R.; Güdel, H. U. *Acc. Chem. Res*. **2000**, *33*, 235.

(27) (a) Ju, J. J.; Kwon, T. Y.; Kim, H. K.; Kim, J. H.; Kim, S. C.; Cha, M.; Yun, S. I. *Mater. Lett*. **1996**, *29*, 13. (b) Fernández, J.; Sanz, M.; Mendioroz, A.; Balda, R.; Chaminade, J. P.; Ravez, J.; Lacha, L. M.; Voda, M.; Arriandiaga, M. A. *J. Alloys Compd.* **2001**, *323*−*324*, 267.

(28) (a) Reinhard, C.; Valiente, R.; Güdel, H. U. *J. Phys. Chem. B* **2002**, *106*, 10051. (b) Gerner, P.; Wenger, O. S.; Valiente, R.; Güdel, H. U. *Inorg. Chem*. **2001**, *40*, 4534.

(29) (a) Vetrone, F.; Boyer, J.-C.; Capobianco, J. A.; Speghini, A.; Bettinelli, M. *J. Phys. Chem. B* **2003**, *107*, 10747. (b) Oomen, E. W. J. L. *Adv. Mater*. **1991**, *3*, 403.

(30) (a) Cockroft, N. J.; Jones, G. D.; Syme, R. W. G. *J. Lumin*. **1989**, *43*, 275. (b) Salley, G. M.; Valiente, R.; Güdel, H. U. *J. Lumin.* **2001**, *94*−*95*, 305. (c) Gamelin, D. R.; Güdel, H. U. *Inorg. Chem.* **1999**, *38*, 5154.

(31) Auzel, F. *Proc. IEEE* **1973**, *61*, 758.

up-conversion through the GSA/ETU process.[32] On the other hand, because the NDC ligand shows no absorption at about 580 nm in the UV−vis spectrum (Figure S9 in the Supporting Information), the excitation wavelength (580 nm) should correspond to the $^4I_{9/2} \rightarrow {}^4G_{5/2}$ transition of the Nd^{III} ions.[27a] On the basis of the crystal structure, a GSA/ETU mechanism is more likely for the up-conversion of our system.[33] However, the possibility of the coexistence of GSA/ETU and GSA/ESA mechanisms in the up-conversion process of **2** cannot be excluded yet.

Magnetic Properties. The temperature-dependent magnetic susceptibility data of compounds **1**, **2,** and **4** have been measured for polycrystalline samples at an applied magnetic field of 1000 Oe in the temperature range of 4−300 K. The plots of $\chi_M T$ and $1/\chi_M$ vs T of the three compounds **1**, **2**, and **4** are shown in Figure 9. For **1**, as the temperature is lowered from room temperature, the $\chi_M T$ value decreases, owing to the depopulation of the Stark levels with nonzero J values for a single Eu^{III} ion (Figure 9a). At the lowest temperature, $\chi_M T$ is close to zero, indicative of a $J = 0$ ground state of the Eu^{III} ion ($^7F_0$).[19b] The magnetic susceptibility above 200 K follows the Curie−Weiss law because of the presence of thermally populated excited states.

In the experimental $\chi_M T$ vs T curve for **2**, there is a decrease in the value of $\chi_M T$ as the temperature is lowered from room temperature to 4 K (Figure 9b). The occurrence of this behavior is attributed to the contribution of the crystal field, which splits the $^4I_{9/2}$ free-ion ground state into five Kramers doublets, interpreted by Kahn and co-workers for the compound $[NdL_2(H_2O)_4](ClO_4)_3 \cdot 4H_2O$, where L = 2-formyl-4-methyl-6-[*N*-(2-pyridylethyl)formimidoyl]-phenol.[34] Considering the large anisotropy of the Nd^{III} system, it is difficult to fit the magnetic data with an accurate model. Nevertheless, in the 50−300 K temperature range, the magnetic susceptibility data of **2** can be described by a Curie−Weiss fitting with $C = 3.05$ cm^3 K mol^{-1} and $\theta = -30.04$ K. The large θ values indicate the importance of ligand-field effects in compound **2**. The nature of the interactions between Ln^{III} ions with a first-order orbital momentum, such as Nd^{III} ions, cannot simply be deduced from the shape of the $\chi_M T$ vs T curve and the θ value alone.[35]

For compound **4**, again the $\chi_M T$ value continuously decreases to almost 0 as T approaches 0 K (Figure 9c), mainly because of the depopulation of the Stark levels with nonzero J values for a single Eu^{III} ion.[19b,36] The magnetic susceptibility of **4** above 240 K follows the Curie−Weiss law because of the presence of thermally populated excited states. It should be pointed out that, because of the complexity of the structures as well as the lack of suitable models, more detailed calculations of the magnetic interactions for **1**, **2**, and **4** seem to be difficult.

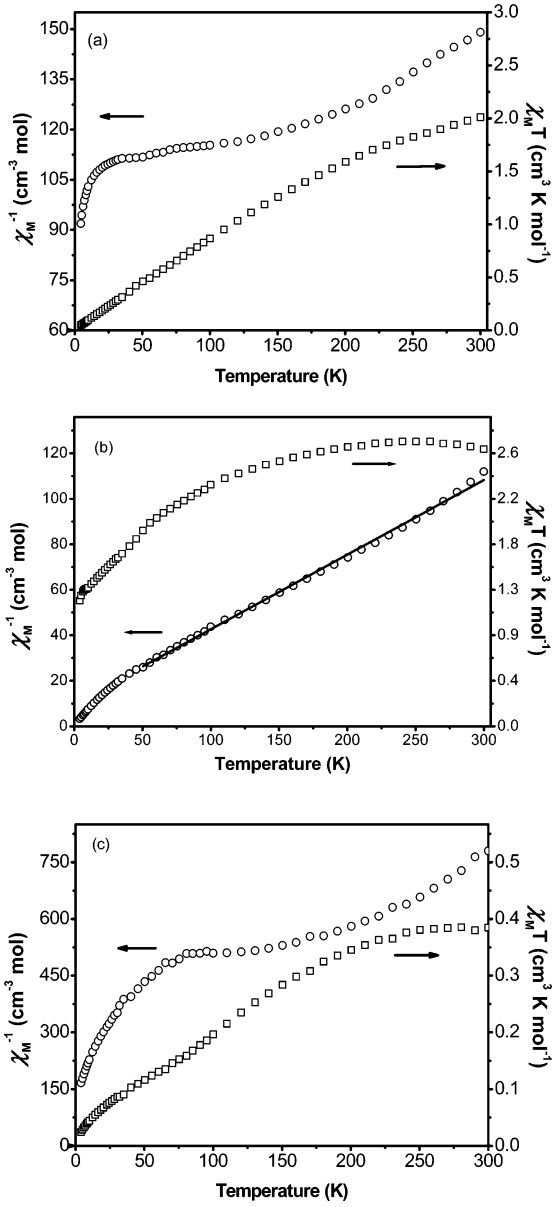

Figure 9. Plots of the temperature dependence of $\chi_M T$ (open squares) and χ_M^{-1} (open circles) for compounds **1** (a), **2** (b), and **4** (c). The solid lines show the best fit to the Curie−Weiss law for **2** in the 50−300 K temperature range.

Conclusions

Through a preheating and cooling-down crystallization technique and in the presence of DMF, four new rare-earth carboxylate materials have been synthesized. This synthetic approach not only reduces the possibility of involvement of coordination water molecules in the compounds but also improves the solubility of aromatic carboxylic acids and therefore the formation of single crystals suitable for structural analysis. The solid-state luminescent spectra demonstrate that compounds **1** and **4** are red luminescent materials potentially useful for optical devices and compound **2** is a good candidate for a near-IR-emitting

(32) Gamelin, D. R.; Wermuth, M.; Güdel, H. U. *J. Lumin.* **1999**, *83*−*84*, 405.
(33) Karbowiak, M.; Edelstein, N. M.; Drożdżyński, J. *J. Lumin.* **2003**, *104*, 197.
(34) Andruh, M.; Bakalbasis, E.; Kahn, O.; Trombe, J. C.; Porcher, P. *Inorg. Chem.* **1993**, *32*, 1616.
(35) Kahn, M. L.; Sutter, J.-P.; Golhen, S.; Guionneau, P.; Ouahab, L.; Kahn, O.; Chasseau, D. *J. Am. Chem. Soc.* **2000**, *122*, 3413.
(36) Wu, C.-D.; Lu, C.-Z.; Yang, W.-B.; Lu, S.-F.; Zhuang, H.-H.; Huang, J.-S. *Eur. J. Inorg. Chem.* **2002**, 797.

application. Furthermore, compound **2** exhibits interesting up-conversion properties with UV and intense blue up-conversion emissions upon 580-nm excitation. The magnetic properties of compounds **1**, **2**, and **4** were also studied by measuring their magnetic susceptibility over the temperature range of 4−300 K. It is anticipated that other new lanthanide carboxylate compounds with interesting structures as well as physical properties may also be synthesized through the preheating and cooling-down crystallization approach.

Acknowledgment. This work was supported by the National Natural Science Foundation of China and the Education Ministry of China.

Supporting Information Available: Four X-ray crystallographic files (CIF), selected bond distances and angles, FTIR spectra, and simulated and experimental powder XRD patterns for compounds **1**−**4** and a UV−vis spectrum for the NDC ligand. This material is available free of charge via the Internet at http://pubs.acs.org.

IC051557O